in vivo *36*: 140-152 (2022)
doi:10.21873/invivo.12685

Transgenic Immortalization of Human Dermal Fibroblasts Mediated Through the MicroRNA/SIRT1 Pathway

WILASINEE PROMJANTUEK, NIPHA CHAICHAROENAUDOMRUNG, RUCHEE PHONCHAI, PHONGSAKORN KUNHORM and PARINYA NOISA

Laboratory of Cell-Based Assays and Innovations, School of Biotechnology, Institute of Agricultural Technology, Suranaree University of Technology, Nakhon Ratchasima, Thailand

Abstract. *Background/Aim: Human dermal fibroblasts (HDFs) are widely used as a skin model in cosmetic and pharmaceutical industry due their advantages for the cosmetic industry and medical aspects. Telomeres are key players in controlling cellular aging, in which telomeres and the telomerase enzyme (hTERT) can maintain proliferative capacity and prolong cellular senescence. The primary aim of the study was to elucidate the underlying mechanisms of hTERT/SV40 immortalization of human dermal fibroblasts. Materials and Methods: Transgenic expression of hTERT and SV40 large antigen, as well as co-transfection of both factors was performed and their significance evaluated in terms of HDF immortalization efficiency. Results: The results showed that the immortalized fibroblasts of all conditions can be cultured in over 60 passages and maintain their telomere length. Further, key markers of skin cells, such as COL1A1, KRT18 and ELASTIN, were up-regulated in immortalized cells. In addition, p53 expression was enhanced in all immortalized cells, in accordance with activation of the SIRT1 gene upon transgenic immortalization. The significant role of SIRT1 in fibroblast proliferation was assessed by shRNA-knockdown, and it was found that SIRT1 silencing led to loss of Ki67, a proliferation marker. Moreover, miR-93, a SIRT1-targeted miRNA, also had a significantly reduced expression in the co-transfected immortalized cells, highlighting the linkage of the miRNA and SIRT1 pathway in the immortalization of human dermal fibroblasts. Conclusion: This evidence from this study could benefit the efficient development of human skin cell lines for use in the cosmetic industry in the future.*

Correspondence to: Parinya Noisa, Ph.D., School of Biotechnology, Institute of Agricultural Technology, Suranaree University of Technology, Nakhon Ratchasima 30000, Thailand. Tel: +66 44223393, Fax: +66 44224154, e-mail: p.noisa@sut.ac.th

Key Words: Human dermal fibroblasts, immortalization, SIRT1, micro-RNA.

The expansion of somatic cells *in vitro* for research and medical applications is limited by their short proliferative lifespan (1). Cellular senescence is a state of irreversible arrest of cell proliferation, exhibiting enlarged morphological changes and senescence-associated heterochromatin foci formation. Senescence, originating from the Latin word '*SENAX*', refers to a physiological program towards permanent cell-cycle arrest. Cellular senescence can be stimulated *via* a variety of factors, such as tumour suppressor proteins, oncogene activation, telomere shortening, genomic DNA damage, and activation of the p53/p21 pathway. Oncogene-induced senescence is a cellular response found in pre-malignant tumours. Senescent cells exert a pleotropic effect on development, tissue aging and regeneration, inflammation, wound healing and tumour suppression (2). Currently, cosmeceutical research is developed to correct skin problems, including skin aging, skin inflammation, skin disorders, and acne. In cosmetics, human skin cells are used as a standard model for demonstrating the therapeutic potential of cosmetic products. The use of *in vitro* tests is a critical step in the development of new products for treating skin problems. The study of human skin cell biology has increased the hope for a successful cell therapy in aesthetic medicine and cosmetics. Various types of skin cells are responsible for synthesizing and organizing the skin with three layers, including (i) epidermis containing keratinocytes, melanocytes and Langerhans cells; (ii) dermis that is populated with fibroblasts, vessels, and dendritic cells and (iii) subcutaneous tissue in the deepest layers (3). HDFs exist in several locations, including the dermal papilla, the hair follicle, the blood capillary and the collagen fibre. HDFs are used to explore wound-healing and aging skin phenomena, which play a pivotal role in maintaining skin function. However, a major bottleneck of using human dermal fibroblasts is their limited proliferative capacity *ex vivo,* and the tendency to undergo senescence (4). In some cases, the cells may overcome this

replication block by virus-suppressed p53 and pRb function. However, continued proliferation results in further shortening of telomeres, extensive chromosome damage and genomic crisis leading to widespread apoptosis (5).

Cellular immortalization is a technique aiming to solve the limits of cellular senescence. Several pathways are implicated in regulating spontaneous cell immortalization and anti-senescence, including loss of tumour suppressors, in particular p53, which is necessary but not sufficient to induce immortalization (6). Telomere shortening has a definitive role in the loss of chromosomal integrity and controls aging of cells during cell division. The telomere is a protein/DNA complex at the end cap of the chromosome, and the maintenance of their length is essential for genomic stability and cell viability (7). Human telomerase reverse transcriptase (hTERT) functions to create immortalized cells by maintaining the length of the telomere. The catalytic protein subunit of telomerase plays a role in controlling the mammalian cell lifespan. Telomerase activation is highly increased in human cancer but reduced in most human somatic cells (8). Besides hTERT, DNA tumour viruses such as simian virus 40 (SV40) large T antigen could directly suppress tumour retinoblastoma protein (pRB) and activate the cell cycle of host cells. The generation of immortalised cell lines by using SV40 large T antigen provides a vital tool to examine the mechanisms of cellular immortalization (8). The extension of the cell lifespan is largely attributed to large T antigen forming complexes with pRB and p53 (9).

A recent study showed that cell proliferation and cellular rejuvenation are also regulated by sirtuin (SIRT) activation (10). SIRT1 plays multiple roles in mammalian cells, since SIRT1-deficient mice suffer multiple abnormalities, including defects in spermatogenesis and in heart and retina development (11, 12). However, the involvement of SIRT1 in cell immortalization process is not well understood. The aim of this study was to establish immortalized human dermal fibroblasts and explore the possible mechanisms underlying cellular immortalization by hTERT and SV40 large T antigen.

Materials and Methods

Chemicals and reagents. The hTERT (pBABE-neo-hTERT) and SV40 large T antigen (pBABE-neo largeTcDNA) plasmid were purchased from Addgene, Cambridge. MA.3-(4,5-dimethyl-2-thiazolyl)-2,5-diphenyl-2H-tetrazolium bromide (MTT), 4,6-diamidino-2-phenylindole (DAPI) and dimethyl sulfoxide (DMSO) were purchased from SIGMA (Roedermark, German). Dulbecco's Modified Eagle's Medium (DMEM) and fetal bovine serum (FBS) were purchased from HyClone (Hyclone, Logan, UT, USA). Trypsin-EDTA (0.05%), L- glutamax and non-essential amino acids were obtained from Gibco (Gibco, Carlsbad, CA, USA). Antibodies against SIRT1, Collagen1 type I and Vimentin were purchased from Merck (Merck KGaA, Darmstadt, Germany).

Cell culture. Human dermal fibroblasts (HDFs) were obtained from cell-based assay and innovation (CBAI), biotechnology, SUT. SHSY-5Y cells were purchased from ATCC (CRL-2266; www.atcc.com). HDFs were stored in liquid nitrogen prior to experimentation. Cells were thawed, washed twice with 1× Phosphate Buffered Saline (1× PBS, pH7.4) and seeded into T25 flask (NEST, Jiangsu, PR China). The cells were cultured in high-glucose Dulbecco's Modified Eagle Medium (DMEM/HG; Hyclone), supplemented with 10% (v/v) fetal bovine serum (FBS; Gibco BRL, Grand Island, NY, USA), 1 mM L-glutamine, 1 mM Minimal Essential Medium (MEM; Sigma-Aldrich, St. Louis, MO, USA), 100 U/ml Penicillin and 100 g/ml Streptomycin (Sigma-Aldrich) and incubated at 37˚C in 5% CO_2 (Thermo Scientific, Waltham, MA, USA).

Plasmid transfection. To immortalize HDFs and increase their cell proliferative capacity, the cells were transfected by plasmid hTERT (pBABE-neo-hTERT; Addgene) and SV40 large T antigen (pBABE-neo largeTcDNA; Addgene). These cells were seeded on 6-well plates at a density of 2.0×10^5 cells per well. When the cells reached 70% confluence, a reagent containing plasmid and Lipofectamine 2000 (Promega, Madison, WI, USA) was added and the plate incubated at 37˚C in 5% CO_2 for 24 h, as mentioned in the manufacturer's protocol (13). After 48 h in culture, the transfected cells were subjected to antibiotic selection with either neomycin or geneticin by adding 300 μg/ml of G418 sulphate (Sigma-Aldrich) into the serum-free medium. G418-resistance cells were isolated and subcultured for expansion.

Cell proliferation. Cell viability and cell proliferation were measured by MTT (3-(4, 5-dimethylthiazolyl-2)-2, 5-diphenyltetrazolium bromide) assay. Approximately 3×10^3 cells were seeded onto 96-well microplates (NEST) and cultured in 10% DMEM for 9 days. Cells were counted every 48 h until day 9. At each time point, the medium was discarded; cells were washed twice with 1× PBS, and 100 μl of 0.5 mg/μl MTT was added and incubated for 2 h at 37˚C in 5% CO_2. After 2 h, the MTT solution was discarded, and 100 μl dimethyl sulfoxide (Sigma-Aldrich) was added to solubilize the formazan crystals. The optical density was measured at 570 nm by a microplate reader (SPECTROstar Nano, BMG Labtech, Offenburg, Germany).

RNA isolation and cDNA synthesis. Total RNA from the cells was extracted by using the NucleoSpin RNA kit (Macherey-Nagel, Dueren, Germany) in accordance with the manufacturer's protocol. On the other hand, miRNAs were extracted from dermal fibroblasts with the miRNeasy mini kit (QIAGEN, Hilden, Germany) in accordance with the manufacturer's protocol. The OD260/280 ratio of the RNA samples was measured, and samples with a ratio above 2.0 were used for reverse transcription. RNA (0.5 mg) was reverse transcribed by using ReverTra Ace®qPCR RT Master Mix with gDNA Remover (Toyobo, Osaka, Japan). The 4× DNA master mix reactions were performed at 65˚C for 5 min, and then 5× RT master mixes were added, and the reactions were performed at 37˚C for 15 min and 98˚C for 5 min.

Reverse-transcription PCR and qPCR. The expression of fibroblast and cell cycle genes was assayed by PCR (Bio-Rad, Hercules, CA, USA) using the primers shown in Table I. Glyceraldehyde-3-phosphate dehydrogenase (*GAPDH*) was used as the internal control gene. PCR

Table I. *List of primers used in this study.*

Gene	Sequence (5'→3')
GAPDH	Forward: 5' TCACCACCACGGCCGAGCG 3'
	Reverse: 5' TCTCCTTCTGCATCCTGTCG 3'
Vimentin	Forward: 5' CCAGGCAAAGCAGGAGTC 3'
	Reverse: 5' CGAAGGTGACGAGCCATT 3'
Elastin	Forward: 5' CCGCTAAGGCAGCCAAGTATGGA 3'
	Reverse: 5' AGCTCCAACCCCGTAAGTAGGAAT 3'
COL1A1	Forward: 5' GGGCAAGACAGTGATTGAATA 3'
	Reverse: 5' ACGTCGAAGCCGAATTCCT 3'
COL3A1	Forward: 5' AGGTCCTGCGGGTAACACT 3'
	Reverse: 5' ACTTTCACCCTTGACACCCTG 3'
p53	Forward: 5' CCCCTCCTGGCCCCTGTCATCTTC 3'
	Reverse: 5' GCAGCGCCTCACAACCTCCGTCAT 3'
P21	Forward: 5' CATGTGGACCTGCACTGTCTTGTA 3'
	Reverse: 5' GAAGATCAGCCGGCGTTTG 3'
SIRT1	Forward: 5' TGCTGGCCTAATAGAGTGGCA 3'
	Reverse: 5' CTCAGCGCCATGGAAAATGT 3'
KRT18	Forward: 5' CAAAGCCTGAGTCCTGTCCTT 3'
	Reverse: 5' CTCCCGGATTTTGCTCTCCA 3'
B-actin	Forward: 5' CTCTGCTCCTCCTGTTCGAC 3'
	Reverse: 5' TTAAAAGCAGCCCTGGTGAC 3'
Tel	Forward: 5' TGTGCACCAACATCTACAAG 3'
	Reverse: 5' GCGTTCTTGGCTTTCAGGAT 3'
Ki67	Forward: 5' TGTATCCTTTGGTGGTCGTCTA 3'
	Reverse: 5' GCTGGAGTGTGAGTGGTGAG 3'
36B4A	Forward: 5' AAG CGC GTC CTG GCA TTG TCT 3'
	Reverse: 5' CCG CAG GGG CAG CAG TGG T 3'
U6	Forward: 5' CGCAAGGATGACACGCAAATTC 3'
miR22	Forward: 5' AAGCTGCCAGTTGAAGAACTGT 3'
miR34a	Forward: 5' TGGCAGTGTCTTAGCTGGTTGT 3'
miR93	Forward: 5' CAAAGTGCTGTTCGTGCAGGTAG 3'
miR217	Forward: 5' CTCAACTGGTGTCGTGGAGTCGG CAATTCAGTTGAGTTGGCATT 3'
miR449	Forward: 5'TGGCAGTGTATTGTTAGCTGGT3'

products were separated by gel electrophoresis (1.5% agarose gel, Vivantis, Selangor Darul Ehsan, Malaysia), and visualized by EtBr staining. The stained gels were detected with a GelDoc system (Gel Doc EZ Imager, Bio-Rad) and the relative gene expression levels measured. The expression levels of *Tel*, *36B4*, *Ki67*, *β-actin*, *U6* and 5 MiRNAs were examined by qPCR using the primers shown in Table I. The QuantStudio 5 Real-Time PCR System (Thermo Scientific) was used to carry out real-time PCR experiments which were conducted in 96-well plates. To monitor cDNA amplification, qPCR BioSyGreen Mix Low-Rox (PCR BIOSYSTEMS, London, UK) was used in a 20 μl reaction volume. Cycling conditions according to the specific SYBR Green protocol were as follows: 95˚C for 30 s, 60˚C for 30 s and 72˚C for 45 s (40 cycles). Melting curve analysis of the PCR products was performed by heating at 60˚C for 60 s, 95˚C for 15 s and continuous measurement of the fluorescence to verify the PCR products. The relative expression was determined by the 2^ (-delta delta C(T)) method with the expression of β-actin as the housekeeping reference gene.

Telomere measurement. DNA was isolated from fibroblasts with the genomic RNA extraction kit (Macherey-Nagel) for telomere measurement. Telomere length was measured as previously described (14) by qPCR amplification with oligonucleotide primers designed to hybridize to the TTAGGG and CCCTAA repeats. For all qPCR reactions, qPCR BioSyGreen Mix Low-Rox (PCR BIOSYSTEMS) was used for both T and S qPCR. The final telomere primer concentrations were as follows: tel 1, 270 nM and tel 2, 900 nM. The final 36B4 (single copy gene) primer concentrations were 36B4u, 300 nM and 36B4d, 500 nM. Primer sequences (5'→3') were as follows (15):
tel 1, GGTTTTTGAGGGTGAGGGTGAGGGTGAGGGTGAGGGT;
tel 2, TCCCGACTATCCCTATCCCTATCCCTATCCCTATCCCTA;
36B4u, CAGCAAGTGGGAAGGTGTAATCC;
36B4d, CCCATTCTATCATCAACGGGTACAA.

All PCRs were performed using the QuantStudio 5 Real-Time PCR System (Thermo Scientific). For telomere PCR, 40 cycles of 95˚C for 15 s and 54˚C for 2 min, and for 36B4 PCR, 40 cycles of 95˚C for 15 s and 58˚C for 1 min were set. For telomere length, the LightCycler® 480 by QuantStudio 5 thermocycler was used to generate the standard curve for each run and to determine the dilution factors of standards corresponding to the T and S amounts in each sample. Absolute quantification results for both T and S were obtained using the Second Derivative Maximum method. The relative telomere length value was expressed as the average duplicate telomere over the average duplicate single copy gene (T/S) ratio. All presented telomere lengths were displayed as a relative level, compared to the non-transfected control HDFs. Standard deviation (SD) was obtained from three replicate values of each HDF sample, and statistical analysis was performed by Student's *t*-test.

Immunofluorescence staining. Cells were cultured on coverslips and fixed with 4% paraformaldehyde (PFA) in 1× PBS for 20 min at room temperature. The fixed cells were washed twice with 1× PBS and non-specific binding blocked with 1% bovine serum albumin (EMD Millipore, Billerica, MA, USA) and 0.2% Triton X-100 in 1× PBS. After incubation for 30 min in blocking solution at 4˚C, the cells were incubated in blocking buffer containing the primary antibody [anti-Collagen1 Type I (1:500; MERCK), anti-SIRT1 (1:200; DSHB, Iowa, IA, USA) and anti-Vimentin (1:500; DSHB)] overnight at 4˚C. The cells were washed in washing solution, supplemented with 0.2% Triton X-100 in 1× PBS. Then, the cells were incubated in the secondary antibody either anti-mouse (1:500; Thermo Scientific) or anti-rabbit (1:500; Thermo Scientific) for 2 h at room temperature. Next, the cells were washed with 1× PBS 5 times for 5 min each, the cell nuclei were stained with 4,6-diamidino-2-phenylindole (DAPI, Sigma-Aldrich) and the coverslips were sealed with nail polish on the on the slides. Slides were observed using a fluorescence microscope (ZOE™ Fluorescent Cell Imager, Bio-Rad Laboratories).

Colony formation. The immortalized HDFs were investigated for tumour formation after plasmid transfection. The soft agar assay could detect colony formation in malignant and tumour cells. The cells were cultured in Dulbecco's Modified Eagle's Medium (DMEM) supplemented with 10% FBS, 1% penicillin, and 1% NEA and incubated at 37˚C in 5% CO_2. The agar base was prepared as a 1% agarose gel and melted in a microwave. The 2× DMEM medium was prepared, containing 20% FBS, 1% L-glutamine, 1% penicillin and 1% NEA. The mix was blended with 1% agarose gel and placed into a 35-mm petri dish. Top agar was prepared from

Table II. *Sequences of shRNA used in this study.*

shRNA	Sequence
shRNA 1	Forward: 5'GATCCCCCTGAAGATGACGTCTTATCCTTTCAAGAGAAGGATAAGACGTCATCTTCAGTTTTTA3'
	Reverse: 5'GGGGACTTCTACTGCAGAATAGGAAAGTTCTCTTCCTATTCTGCAGTAGAAGTCAAAAATTCGA3'
shRNA 2	Forward: 5'GATCCCCAACAAATCATAGTGTAATAATTTCAAGAGAATTATTACACTATGATTTGTTTTTTTA3'
	Reverse: 5'GGGTTGTTTAGTATCACATTATTAAAGTTCTCTTAATAATGTGATACTAAACAAAAAAATTCGA3'

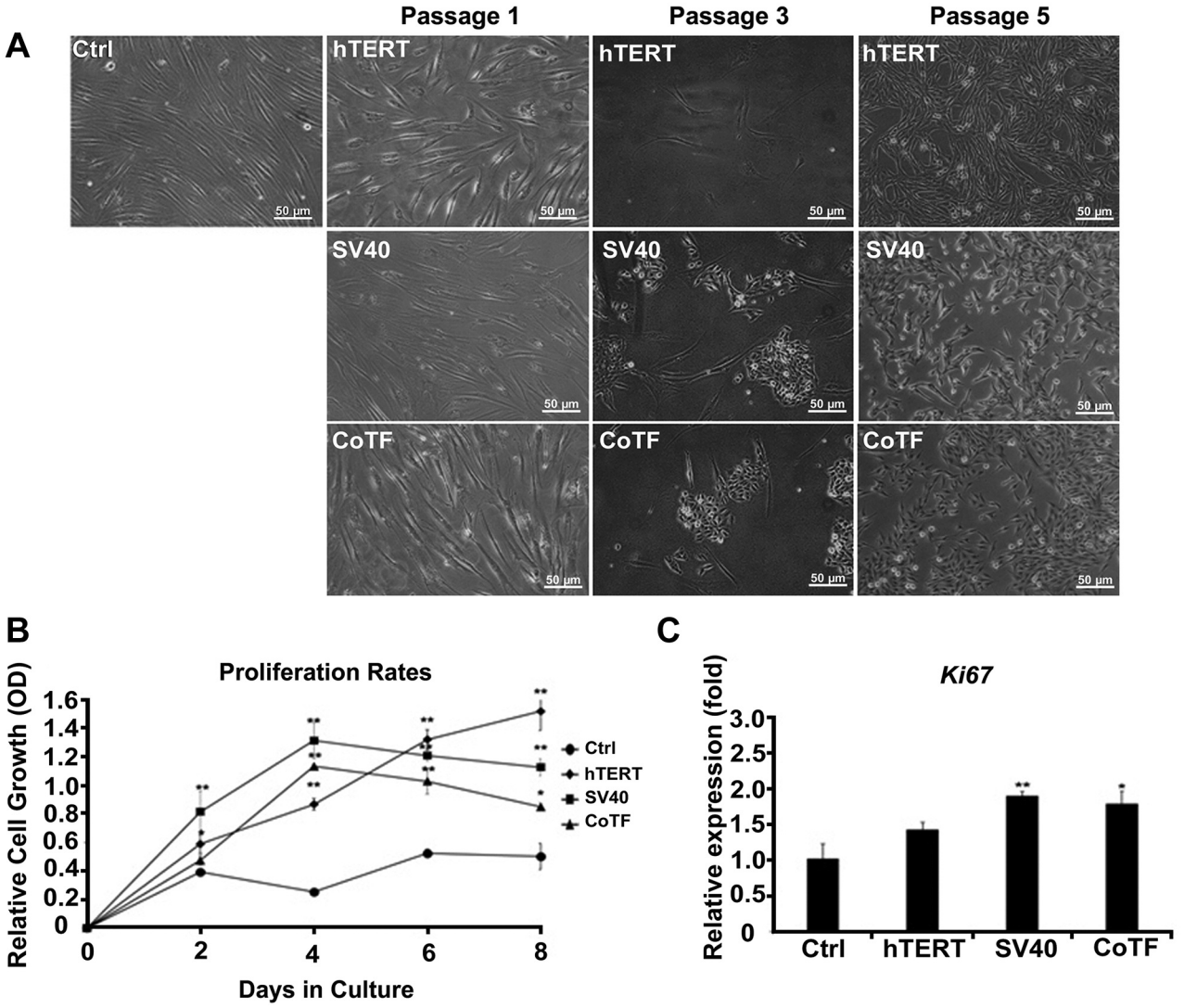

Figure 1. *Continued*

0.3% agarose gel mixed with 2X DMEM and 20% FBS. The immortalized cells were counted and ~5000 cells/plate blended into the 2X DMEM solution. The cells were then transferred onto the base agar and incubated at 37˚C 5% CO_2 for 10-30 days. During the incubation, the cells were seeded on the top agar every 5 days. When the incubation was completed, the soft agar was stained with 0.005% crystal violet for 1 h at room temperature and the number of colonies counted using a microscope (Nikon, Japan).

shRNA preparation and vector amplification. The oligonucleotide was designed by using the basic local alignment search tool (NCBI database, https://blast.ncbi.nlm.nih.gov/Blast.cgi) as shown in

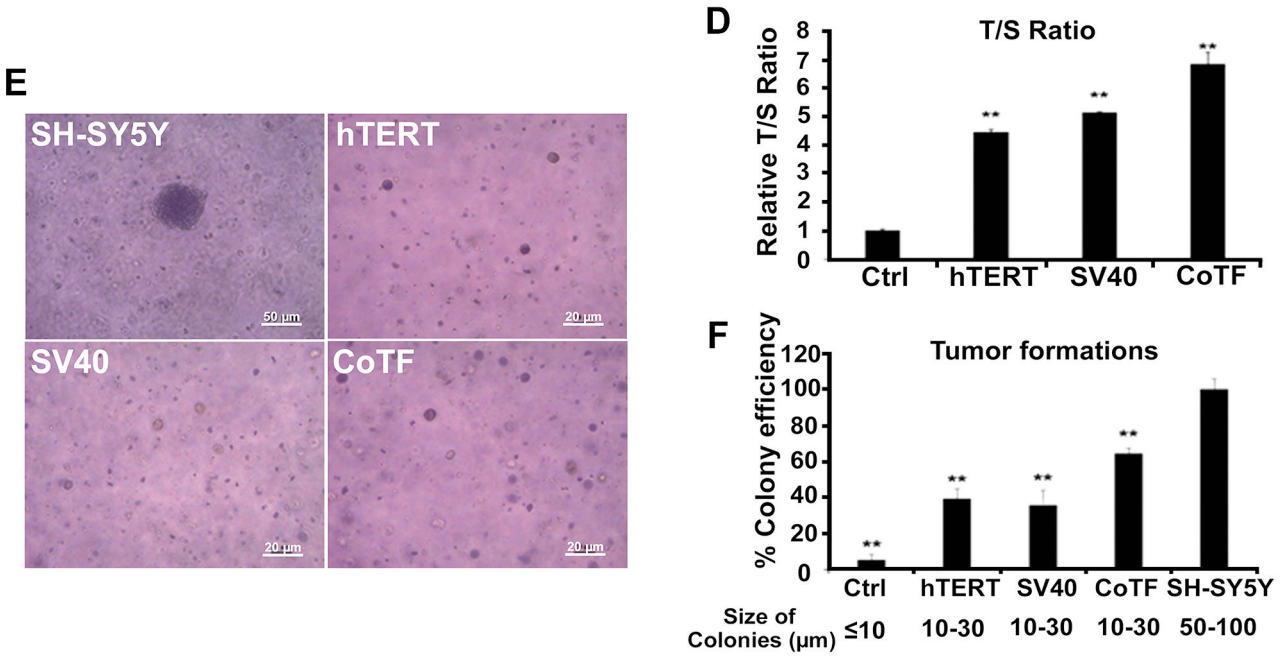

Figure 1. *Immortalized dermal fibroblasts increase cell proliferation and maintain telomere length. (A) Morphology of human dermal fibroblasts (Ctrl), hTERT, SV40 and CoTF in passages 1, 3 and 5. (B) The relative cell proliferation of the immortalized cells by at days 0, 2, 4, 6 and 8. Values were expressed as mean±SD (n=3). *p<0.05 and **p<0.01 versus the control cells. (C) The relative expression of Ki67 by qPCR, compared to the β-Actin gene. Values are expressed as mean±SD (n=3). *p<0.05 and **p<0.01 versus control cells. (D) The relative ratio of the telomere versus 36B4 single copy gene (T/S ratio) by qPCR. Values are expressed as mean±SD (n=3). **p<0.01 versus the control cells. (E) The morphology of tumour formation of the immortalized cells versus SH-SY5Y cells; neuroblastoma was used as a positive control. (F) The percentage of colony-forming efficiency and average size of the tumour. Values are expressed as mean±SD (n=3). *p<0.05 and **p<0.01 versus SH-SY5Y cells.*

Table II. The pSUPERIOR.neo vector (OligoEngine, Seattle, WA, USA) was used for inserting oligonucleotides (shRNA1 and shRNA2), of which the 5' ends corresponded to the BglII site, and the 3' ends contained the *HindIII* corresponding nucleotides. The oligonucleotides were annealed in annealing buffer at 90˚C for 4 min, then at 70˚C for 10 min, prior to cooling the annealed oligonucleotide to 10˚C. Then, the vector was linearized with the BglII and HindIII restriction enzymes (NEW ENGLAND BioLabs; NEB, MA, USA) at 37˚C for 3 h and heat inactivated at 80˚C for 20 min. To ligate the vector, the oligonucleotide to pSUPRIOR vector ratio was 3:1, which was incubated in T4 DNA ligase buffer (NEB) at 37˚C for 10 min and 65˚C for 10 min. The ligation products were amplified by transformation into DH5α competent cells and incubated on ice for 30 min, then heat shocked at 42˚C for 50 s and recovered on ice for 2 min. The mixture was added to LB broth and shaken at 200 rpm and 37˚C for 60 min, prior to spreading onto LB agar plates containing ampicillin and incubating at 37˚C for 16 h. The colonies on agar were selected and picked up into LB broth containing ampicillin for further selection. The plasmid was extracted using a plasmid extraction kit (GF-1 plasmid DNA extraction kit, Vivantis, Malaysia).

Statistical analysis. All experiments were performed in triplicate, and data were expressed as mean±standard deviation (16). Statistical analysis was performed using SPSS (version 16.0, SPSS Inc., Chicago, IL, USA). Significant differences between treatment effects were determined by one-way *ANOVA*, followed by Student's *t*-tests, and *$p<0.05$, **$p<0.01$ and ***$p<0.001$ were considered as statistically significant.

Results

We first examined proliferative capacity and telomere length of the immortalized HDFs. HDFs were successfully immortalized by plasmid transfection of hTERT plasmid and SV40 large T antigen plasmid (SV40) and by co-transfection of both plasmids (CoTF). The cells could be cultured for over 60 passages after transfection. The non-transfected HDFs presented a spindle-shaped morphology with an approximate size of 100-150 µm, while all the transfected cells appeared clumped and were reduced in cytoplasmic volume (Figure 1A). The proliferative capacity of the immortalized cells was demonstrated by the MTT assay and the expression of the proliferation marker Ki67. Notably, all groups of immortalized cells increased their proliferation at days 2 and 4, and the highest rate was found in hTERT-HDFs at days 6 and 8 (Figure 1B). This primary observation suggested that the transfection of hTERT and SV40 could enhance HDF proliferative capacity. The level of *Ki67* gene

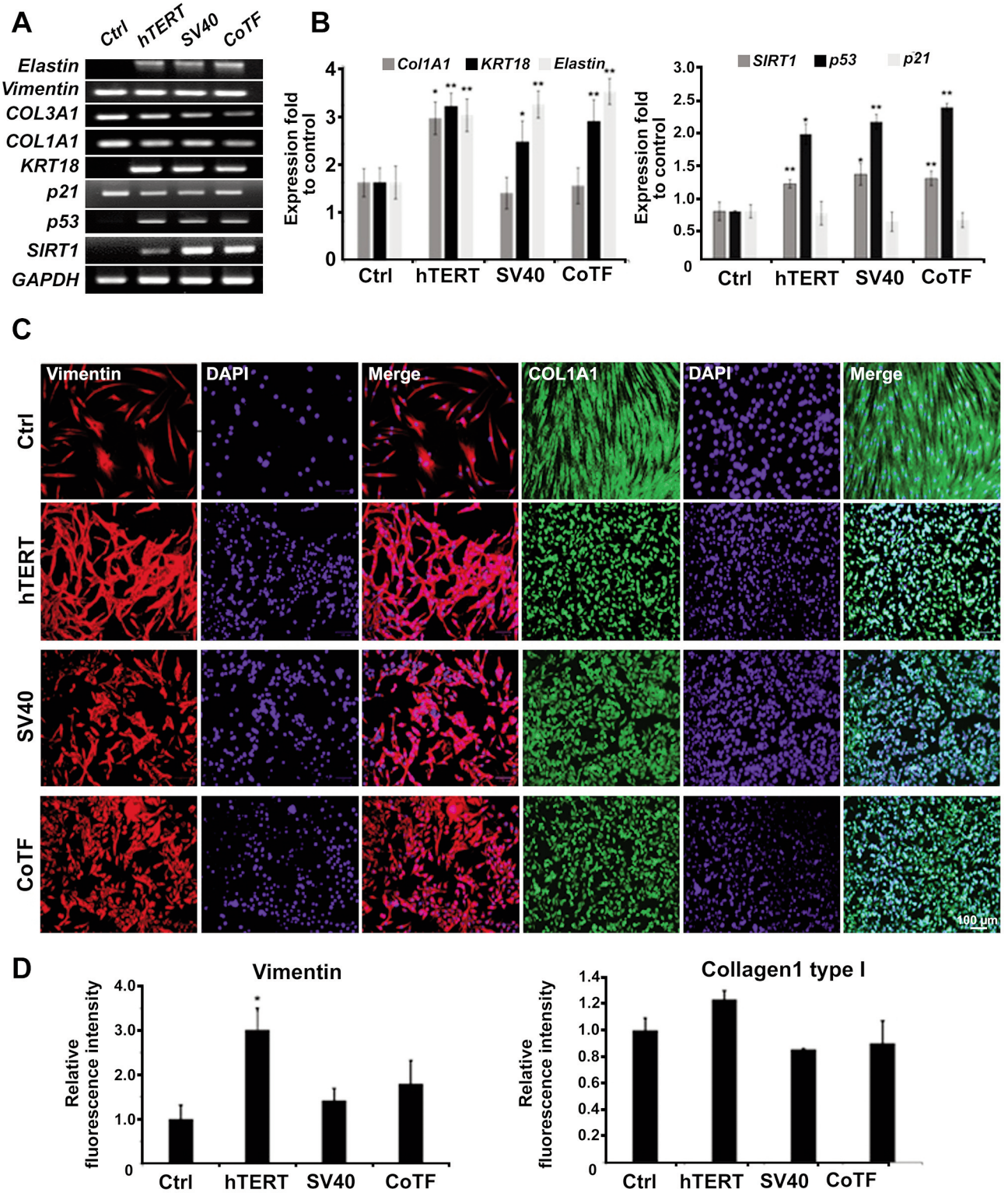

Figure 2. *Characterization of immortalized dermal fibroblasts. (A) PCR results of SIRT1, p53, p21, KRT18, COL1A1, COL3A1, Vimentin, Elastin and GAPDH. (B) Relative expression of COL1A1, KRT18, Elastin, SIRT1, p53 and p21. Values are expressed as mean±SD (n=3). *p<0.05 and **p<0.01 versus the control cells. (C) Immunofluorescence of protein expression of Vimentin and COL1A1 in the immortalized HDFs and the control cells. (D) Relative fluorescence intensity of COL1A1 and Vimentin, calculated from total area of immunofluorescence. Values are expressed as mean±SD (n=3). *p<0.05 versus the control cells.*

expression was used to validate the cell proliferative capacity. Ki67 is a nuclear protein, expressed in all proliferating vertebrate cells, and is widely used as a predictive marker of tumour cell proliferation and growth (17). Ki67 was significantly up-regulated in hTERT, SV40 and CoTF, compared with the control HDFs (Figure 1C). The high expression of *Ki67* gene in SV40- and Co-transfected cells indicated a pivotal function of SV40 in activating human dermal fibroblast proliferation. The correlation of declining cell proliferation and telomere erosion led to the assessment of the T/S ratio, which is measured as telomere length relative to the standard reference DNA. The relative length of the telomere/single (T/S) copy gene of hTERT, SV40 and CoTF HDFs was significantly improved over the control HDFs (Figure 1D). This suggested that ectopic expression of hTERT and SV40 could elongate and maintain the telomere length of HDFs. Anchorage-independent growth is the ability of transformed cells to grow independently of a solid surface and is a hallmark of carcinogenesis. The soft agar colony formation assay was herein used to evaluate cellular transformation *in vitro* of the immortalized HDFs (18). The anchorage-independent growth of the transfected HDFs was compared with human neuroblastoma SH-SY5Y cells, a cancerous cell line used as a positive control (Figure 1E, F). After SH-SY5Y cells were seeded for over 20 days, the colonies grew on agar to an approximate size of 60-100 μm, while the non-transfected control HDFs formed colonies less than 10 μm in diameter. All transfected cells appeared as colonies approximately 10-20 μm in diameter, and their colony formation efficiencies were significantly less than that of SH-SY5Y cells. However, the colony formation efficiency of the transfected HDFs was clearly higher than that of control HDFs, implying the existence of cellular transformation in the immortalized HDFs to a certain degree.

Next, gene and protein expression of the control and the transfected HDFs were assessed by reverse transcriptase PCR and immunofluorescence, respectively. The key fibroblastic makers, including *ELASTIN*, *Vimentin*, *COL3A1*, *COL1A1* and *KRT18*, were determined (19). The expression of *Vimentin*, *COL3A1* and *COL1A1* was at a similar level in the control and transfected HDFs; however, *KRT18* and *ELASTIN* were radically up-regulated in all of the transfected HDFs. This suggested the maintenance and improvement of typical dermal fibroblast property of the immortalized HDFs (Figure 2A and B). Protein levels of vimentin and COL1A1 confirmed the fibroblastic property of the immortalized HDFs (Figure 2C and D). Moreover, the expression of tumour suppressor and anti-aging genes (*RB*, *p21*, *p53* and *SIRT1*) was also evaluated to monitor the state of cellular senescence (16, 20). The direct target of SV40 large T antigen is tumour suppressor RB (pRb). Nevertheless, the expression of *RB* was not detected (not shown in results), but *p53* was significantly increased in all immortalized HDFs. However, the high expression of *p53* is not in accordance with the level of *p21*. *SIRT1*, an anti-aging gene, was investigated in this study to connect its importance to the immortalization process. SIRT1 is important for various cellular processes, including regulation of p53, cell-cycle regulation, and life span extension (21). High expression of *SIRT1* was found in the immortalized HDFs, but not in control cells (Figure 2A and B). The corelation of *p53* and *SIRT1* was prompting further study of the relevance of SIRT1 in cellular immortalization by hTERT/SV40 transgenesis.

Table III. *List of miRNAs involving SIRT1 and cellular senescence pathway. Five miRNAs, which targeted SIRT1 activity, were selected and assessed regarding their involvement in the immortalization of HDFs.*

miRNAs	Tissue/cells/ diseases	Regulation/ function
miR-22	Fibroblast and cancer	Inhibition of growth and metastasis, senescence
miR-217	Endothelial cell	Senescence
miR-34a	Pancreatic cancer, Colorectal cancer, Brain and liver cancer	Neural differentiation, senescence, Liver metabolism
miR-93	Liver	Senescence
miR-449	Gastric cancer	Apoptosis, senescence

Importantly, SIRT1 was found abundantly expressed in all immortalized cells, compared to control HDFs (Figure 3A and B). The relative fluorescence intensity of SIRT1-positive cells was significantly high in hTERT/SV40 transgenic cells. The significance of SIRT1 in cell proliferative capacity was examined by small hairpin RNA (shRNA). SIRT1 was independently knocked-down in HDFs by two shRNAs. Immunofluorescence of SIRT1 was used to confirm the success of SIRT1 gene silencing. The relative fluorescence intensity of both SIRT1-shRNA was significantly reduced, compared to that of the normal control HDFs (Figure 3C and D). Importantly, *Ki67* was found to decrease the expression in the SIRT1-knockdown HDFs (Figure 3E). The influence of SIRT1 on cell proliferation was further verified by using small molecules, resveratrol (SIRT1 activator) and sirtinol (SIRT1 inhibitor). Resveratrol and sirtinol at 1 and 5 μM were applied to the control HDFs for 24 h prior to examining *SIRT1* expression. *SIRT1* was significantly up-regulated by 1 μM resveratrol and down-regulated by 5 μM resveratrol sirtinol, respectively (Figure 3F). The adjustment of *SIRT1* expression by small molecules directly reflected the level of *Ki67* expression (Figure 3H). This evidence indicated the involvement of SIRT1 in the hTERT/SV40 immortalization process.

It is noted that miRNAs are involved in cell proliferation and senescence. Five miRNAs, which targeted SIRT1

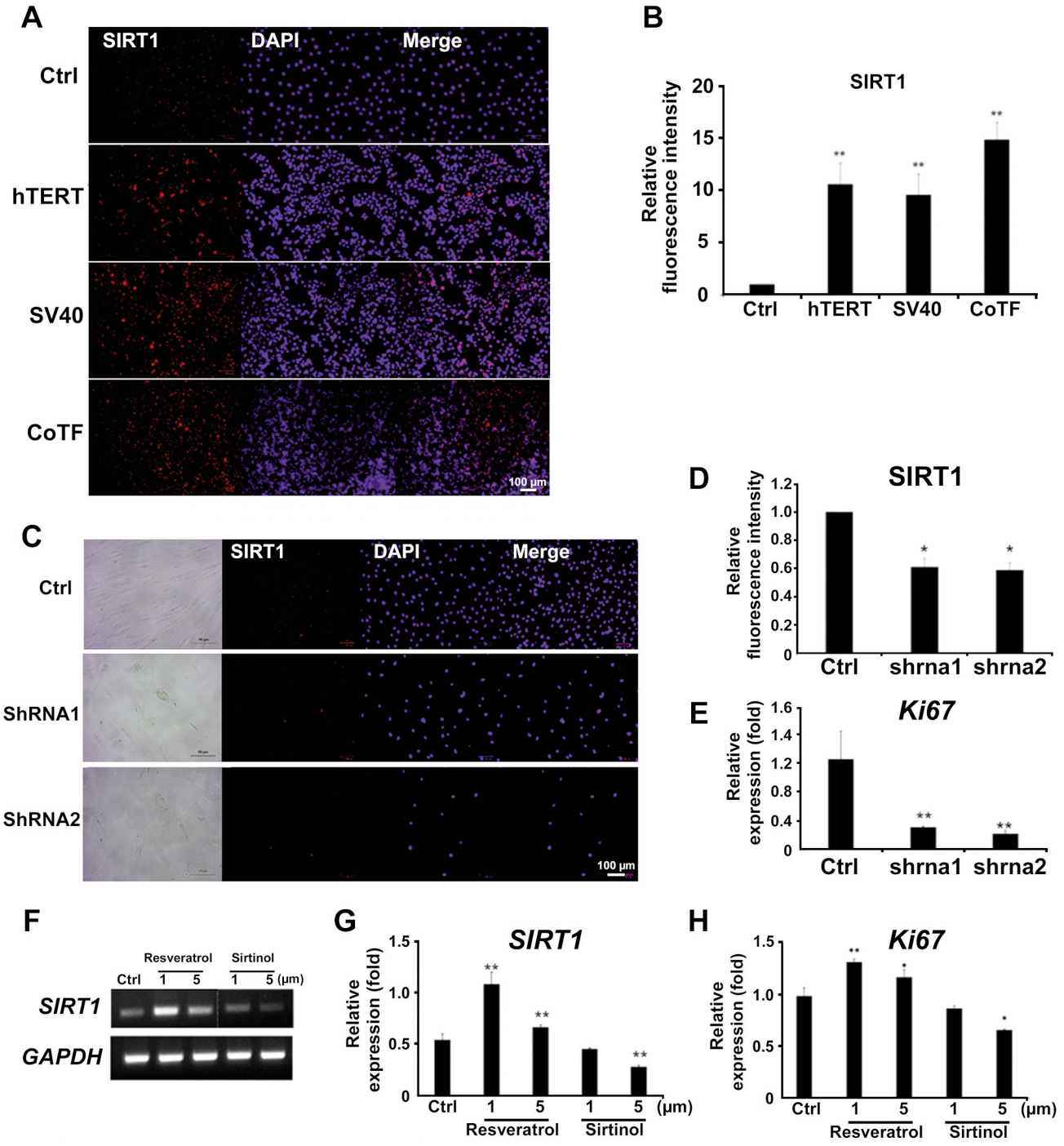

Figure 3. *SIRT1 involved in the immortalization of HDFs. (A) Immunofluorescence of protein expression of SIRT1 in the control (ctrl) and immortalized HDFs (hTERT, SV40 and CoTF). (B) Relative fluorescence intensity of SIRT1-positive cells was quantified by the ImageJ software. Data were presented as mean±SD. **p<0.01 versus control cells. (C) Morphology of SIRT1-knockdown HDFs and immunofluorescence of SIRT1 protein. (D) The relative fluorescence intensity of SIRT1-positive cells, comparing shRNA1 and shRNA2-transfected cells with the non-transfected control cells. Data were quantified by ImageJ and presented as mean±SD. *p<0.05 versus control cells. (E) The relative expression of Ki67 of shRNA1, shRNA2 and control HDFs was compared by RT-PCR. Data are presented as mean±SD. **p<0.01 versus control cells. (F) Effects of resveratrol and sirtinol on SIRT1 expression after treatment at 1 and 5 μM. (G) Relative expression of SIRT1 after treatment with resveratrol and sirtinol at concentration 1 and 5 μM for 24 h. Data are presented as mean±SD. **p<0.01 versus the untreated control cells. (H) The relative expression of Ki67 in normal HDFs after treatment with resveratrol and sirtinol at concentrations of 1 and 5 μM. Data were presented as mean±SD. *p<0.05 and **p<0.01 versus untreated control cells.*

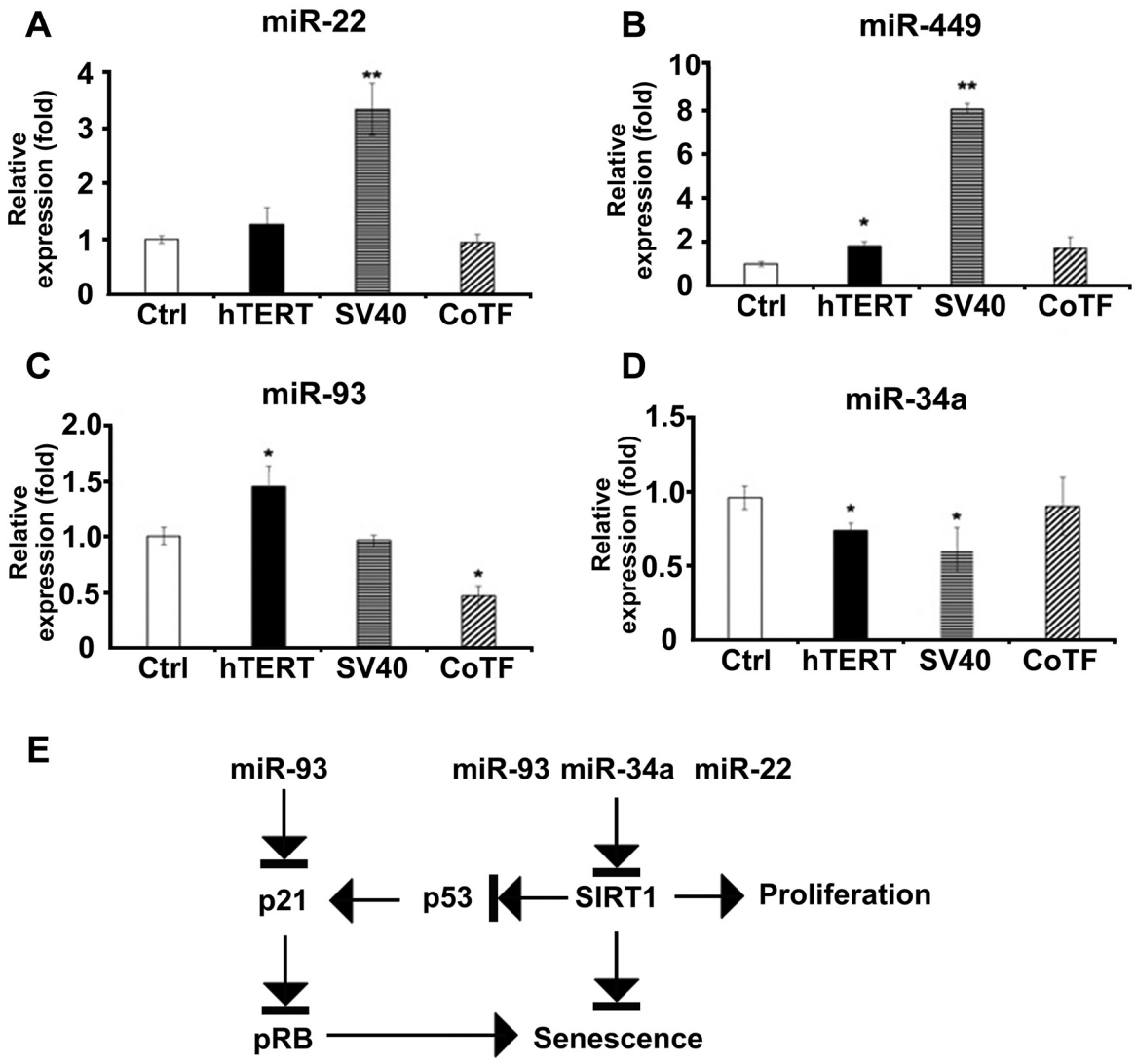

Figure 4. *miRNAs might be involved in SIRT1 activity. (A) Relative expression of miR-22, (B) miR-449, (C) miR-93 and (D) miR-34a. Values were expressed as mean±SD (n=3). *p<0.05 and **p<0.01 versus control HDF2. (E) Flowchart of the predicted microRNAs and their direct targets.*

activity, were selected and assessed regarding their involvement in the immortalization of HDFs (Table III). Four miRNAs were later selected for further analysis by qPCR due to their association with cellular senescence. It was reported that miR-22, miR-449, miR-93 and miR-34a were highly expressed during cellular senescence and aging (22-24). miR-22 and miR-449 were significantly up-regulated in the SV40-transfected HDFs, but not hTERT and CoTF HDFs (Figure 4A and B). On the other hand, the expression level of miR-93 was significantly enhanced in the hTERT-immortalized HDFs, while the level of miR-34a was reduced in both hTERT- and SV40-immortalized HDFs (Figure 4C and D). The down-regulation of miR-34a might associate with the increase in cell proliferation and cell-cycle progression by targeting the *p53* gene (25). Interestingly, the hTERT/SV40 co-transfected HDFs maintained a low level of all studied miRNAs. The possible pathway of the predicted miRNAs and SIRT1 in hTERT/SV40 immortalization was illustrated in Figure 4E.

Discussion

The definition of cellular immortalization is to overcome two growth barriers in culture, senescence and crisis. Senescence is a poorly understood phenomenon exhibited by non-immortal cells in culture, characterized by an exit from the cell cycle and shortening of telomere length (26). In this study, human dermal fibroblasts (HDFs) were

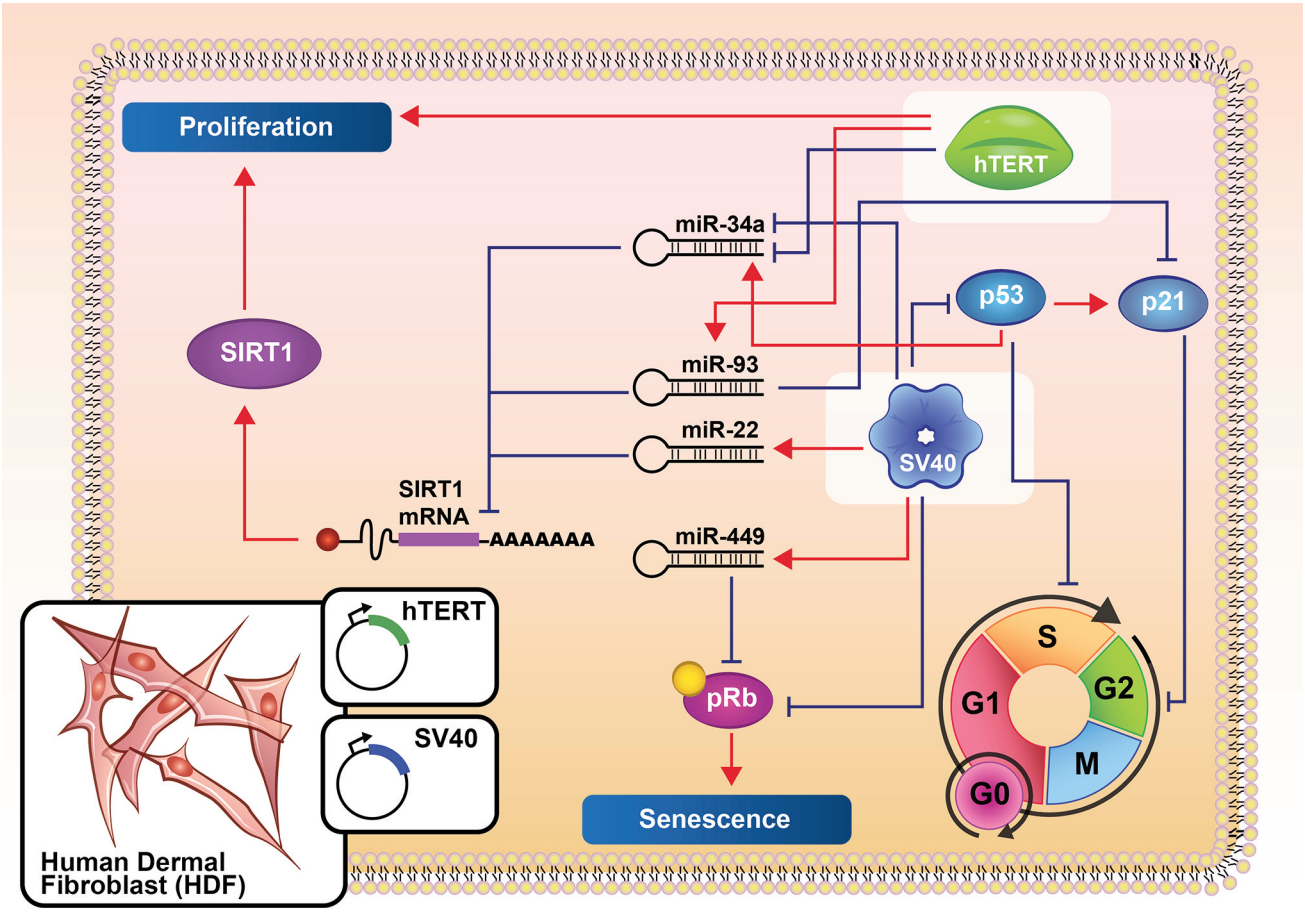

Figure 5. *Graphical illustration of immortalization pathway of human dermal fibroblasts.*

immortalized by using hTERT and SV40 large T antigen, in which both factors could immortalize the cells by controlling the cell cycle and preventing telomere erosion (27-29). hTERT and hTERC protein direct the elongation and metabolism of telomere, and they are widely implemented to immortalize various types of human cell lines (27, 30, 31). hTERT enabled immortalization not only of somatic cells, but also of stem cells. The hTERT-immortalized stem cells were able to maintain their differentiation capacity as well as the expression of stem cell-related cell surface markers (32). SV40 large T antigen is a tumour virus and acts as a suppressor of pRB and p53 to activate cell-cycle arrest (13, 33). The generation of an immortalised cell line by using SV40 large T antigen provides a vital tool to examine the mechanism of cell immortalization (34). The immortalized HDFs in all conditions increased their cell proliferation and maintained telomere length. *Ki67*, a marker of cell proliferation, was up-regulated in hTERT/SV40-transfected cells. Moreover, the anchorage-independent growth assay suggested that the immortalized HDFs by hTERT/SV40 were not transformed into cancer cells (18). The lack of transformation in the transfected HDFs could result by the function of hTERT in circumventing telomere-controlled senescence and SV40 in cell-cycle regulation without inducing global chromosomal instability.

Key dermal fibroblast markers, including *COL1A1*, *COL3A1*, *Elastin* and *Vimentin*, were constantly expressed in the immortalized HDFs, indicating the maintenance of the typical fibroblast property, and the potential application in studying skin biology (35). On the other hand, *SIRT1* and *p53* were highly expressed in transfected HDFs, which suggests their involvement in cell immortalization. SIRT1 regulates many physiological functions, including cell senescence, gene transcription, energy balance and oxidative stress (36), while p53 plays a role in the cell cycle and suppresses tumour formation (37). The SIRT1 level was enhanced in immortalized cells, and the silencing of SIRT1

led to cellular senescence, supporting the hypothesis that SIRT1 might mediate the process of cellular immortalization by hTERT/SV40 in this study. In some other cells, SIRT1 inhibits cellular apoptosis in response to genotoxic stress and may accomplish this by several mechanisms. For instance, SIRT1 deacetylated the p53 tumour suppressor protein, which then down-regulates *p53 via* effects on stability and activity (38, 39). Similarly, the overexpression of SIRT1 inhibited oncogene-induced premature senescence in mouse embryonic fibroblasts (39).

miRNAs are small non-coding RNAs of approximately 22 nucleotides, which play important roles in controlling gene activity (40). Several miRNAs could directly control SIRT1 activity and were predicted to be involved in the hTERT/SV40 immortalization process. miR-93, in particular, was found to directly regulate *SIRT1* transcripts and be involved in cell growth and survival (41, 42). miR-93 expression was significantly decreased in the hTERT/SV40 transfected HDFs, while SIRT1 was upsurged in this cell type. Likewise, the expression of SIRT1 was previously found to be reduced inversely to upregulation miR-93 during aging (23). Besides SIRT1, miR-93 also targeted a number of genes that were involved in cell proliferation, for instance TGF-β1, c-Ski, E2F1 and FOXA1 (43-45). The changes in expression of specific miRNAs might be satisfied for the natural and spontaneous immortalization of human cells, and the role of miRNAs in cellular immortalization still needs further investigation (Figure 4E). This study offered the prospect of creating immortalized human dermal fibroblasts exclusively through the modification of the miRNA/SIRT1 pathway. The activation of the endogenous immortalization pathway could accelerate a spontaneous immortalization process, avoiding cellular transformation. These cells, as they are immortalized and not malignant, could dissect the important issues related to the biology of human skin. The complete image of the immortalization process for human dermal fibroblasts might accelerate the development of an advanced *in vitro* model for skin therapy and cosmetic product production, for instance construction of artificial skin.

In conclusion, cellular immortalization could benefit the efficient development of human cell lines, and accelerate the development of cosmeceutical products. hTERT/SV40 immortalized human dermal fibroblasts were comparable to the primary cells, regarding biological relevance, but without the limitation of proliferation. Using the well-characterized hTERT/SV40-immortalized cells, this study created a reliable cell model for toxicological studies on the skin, which could substitute to animal testing. The immortalized human dermal fibroblasts by transgenic expression of hTERT/SV40 preserved the typical skin cell properties with telomere maintenance, and the immortalization process was connected with the miRNA/SIRT1 pathway (Figure 5).

Conflicts of Interest

The Authors declare that they have no conflicts of interest.

Authors' Contributions

Wilasinee Promjantuek provided the concept and design of the study, performed the experiments, analysed and interpreted data and prepared the article for publication. Nipha Chaicharoenaudomrung analysed and interpreted the data and prepared the article for publication. Ruchee Phonchai performed experiments, provided resources and prepared the article for publication. Phongsakorn Kunhorm analysed and interpreted data and prepared the article for publication. Parinya Noisa provided the concept and design of the study, collected samples, analysed and interpreted data, wrote the manuscript, prepared the article for publication and gave the final publication approval of the manuscript.

Acknowledgements

This work was supported by Suranaree University of Technology (SUT) Research and Development Fund.

References

1 Petkov S, Kahland T, Shomroni O, Lingner T, Salinas G, Fuchs S, Debowski K and Behr R: Immortalization of common marmoset monkey fibroblasts by piggyBac transposition of hTERT. PLoS One *13(9)*: e0204580, 2018. PMID: 30261016. DOI: 10.1371/journal.pone.0204580

2 Wang AS and Dreesen O: Biomarkers of cellular senescence and skin aging. Front Genet *9*: 247, 2018. PMID: 30190724. DOI: 10.3389/fgene.2018.00247

3 Yousef H, Alhajj M and Sharma S: Anatomy, Skin (Integument), Epidermis. 2021. PMID: 29262154.

4 Yoon JE, Kim Y, Kwon S, Kim M, Kim YH, Kim JH, Park TJ and Kang HY: Senescent fibroblasts drive ageing pigmentation: A potential therapeutic target for senile lentigo. Theranostics *8(17)*: 4620-4632, 2018. PMID: 30279727. DOI: 10.7150/thno.26975

5 Jafri MA, Ansari SA, Alqahtani MH and Shay JW: Roles of telomeres and telomerase in cancer, and advances in telomerase-targeted therapies. Genome Med *8(1)*: 69, 2016. PMID: 27323951. DOI: 10.1186/s13073-016-0324-x

6 Fridman AL and Tainsky MA: Critical pathways in cellular senescence and immortalization revealed by gene expression profiling. Oncogene *27(46)*: 5975-5987, 2008. PMID: 18711403. DOI: 10.1038/onc.2008.213

7 O'Sullivan RJ and Karlseder J: Telomeres: protecting chromosomes against genome instability. Nat Rev Mol Cell Biol *11(3)*: 171-181, 2010. PMID: 20125188. DOI: 10.1038/nrm2848

8 Holysz H, Lipinska N, Paszel-Jaworska A and Rubis B: Telomerase as a useful target in cancer fighting-the breast cancer case. Tumour Biol *34(3)*: 1371-1380, 2013. PMID: 23558965. DOI: 10.1007/s13277-013-0757-4

9 Lin JY and Simmons DT: The ability of large T antigen to complex with p53 is necessary for the increased life span and partial transformation of human cells by simian virus 40. J Virol *65(12)*: 6447-6453, 1991. PMID: 1658353. DOI: 10.1128/JVI.65.12.6447-6453.1991

10 Rajamohan SB, Pillai VB, Gupta M, Sundaresan NR, Birukov KG, Samant S, Hottiger MO and Gupta MP: SIRT1 promotes cell survival under stress by deacetylation-dependent deactivation of poly(ADP-ribose) polymerase 1. Mol Cell Biol *29(15)*: 4116-4129, 2009. PMID: 19470756. DOI: 10.1128/MCB.00121-09

11 Cheng HL, Mostoslavsky R, Saito S, Manis JP, Gu Y, Patel P, Bronson R, Appella E, Alt FW and Chua KF: Developmental defects and p53 hyperacetylation in Sir2 homolog (SIRT1)-deficient mice. Proc Natl Acad Sci U.S.A. *100(19)*: 10794-10799, 2003. PMID: 12960381. DOI: 10.1073/pnas.1934713100

12 McBurney MW, Yang X, Jardine K, Bieman M, Th'ng J and Lemieux M: The absence of SIR2alpha protein has no effect on global gene silencing in mouse embryonic stem cells. Mol Cancer Res *1(5)*: 402-409, 2003. PMID: 12651913.

13 Rathi AV, Sáenz Robles MT, Cantalupo PG, Whitehead RH and Pipas JM: Simian virus 40 T-antigen-mediated gene regulation in enterocytes is controlled primarily by the Rb-E2F pathway. J Virol *83(18)*: 9521-9531, 2009. PMID: 19570859. DOI: 10.1128/JVI.00583-09

14 Cawthon RM: Telomere measurement by quantitative PCR. Nucleic Acids Res *30(10)*: e47, 2002. PMID: 12000852. DOI: 10.1093/nar/30.10.e47

15 Mondello C, Petropoulou C, Monti D, Gonos ES, Franceschi C and Nuzzo F: Telomere length in fibroblasts and blood cells from healthy centenarians. Exp Cell Res *248(1)*: 234-242, 1999. PMID: 10094830. DOI: 10.1006/excr.1999.4398

16 Sdek P, Zhang ZY, Cao J, Pan HY, Chen WT and Zheng JW: Alteration of cell-cycle regulatory proteins in human oral epithelial cells immortalized by HPV16 E6 and E7. Int J Oral Maxillofac Surg *35(7)*: 653-657, 2006. PMID: 16513324. DOI: 10.1016/j.ijom.2006.01.017

17 Li LT, Jiang G, Chen Q and Zheng JN: Ki67 is a promising molecular target in the diagnosis of cancer (review). Mol Med Rep *11(3)*: 1566-1572, 2015. PMID: 25384676. DOI: 10.3892/mmr.2014.2914

18 Paoli P, Giannoni E and Chiarugi P: Anoikis molecular pathways and its role in cancer progression. Biochim Biophys Acta *1833(12)*: 3481-3498, 2013. PMID: 23830918. DOI: 10.1016/j.bbamcr.2013.06.026

19 Satelli A and Li S: Vimentin in cancer and its potential as a molecular target for cancer therapy. Cell Mol Life Sci *68(18)*: 3033-3046, 2011. PMID: 21637948. DOI: 10.1007/s00018-011-0735-1

20 Sung JY, Kim SG, Kim JR and Choi HC: SIRT1 suppresses cellular senescence and inflammatory cytokine release in human dermal fibroblasts by promoting the deacetylation of NF-κB and activating autophagy. Exp Gerontol *150*: 111394, 2021. PMID: 33965557. DOI: 10.1016/j.exger.2021.111394

21 Borra MT, Smith BC and Denu JM: Mechanism of human SIRT1 activation by resveratrol. J Biol Chem *280(17)*: 17187-17195, 2005. PMID: 15749705. DOI: 10.1074/jbc.M501250200

22 Xu D, Takeshita F, Hino Y, Fukunaga S, Kudo Y, Tamaki A, Matsunaga J, Takahashi RU, Takata T, Shimamoto A, Ochiya T and Tahara H: miR-22 represses cancer progression by inducing cellular senescence. J Cell Biol *193(2)*: 409-424, 2011. PMID: 21502362. DOI: 10.1083/jcb.201010100

23 Li N, Muthusamy S, Liang R, Sarojini H and Wang E: Increased expression of miR-34a and miR-93 in rat liver during aging, and their impact on the expression of Mgst1 and Sirt1. Mech Ageing Dev *132(3)*: 75-85, 2011. PMID: 21216258. DOI: 10.1016/j.mad.2010.12.004

24 Zheng Y and Xu Z: MicroRNA-22 induces endothelial progenitor cell senescence by targeting AKT3. Cell Physiol Biochem *34(5)*: 1547-1555, 2014. PMID: 25323119. DOI: 10.1159/000366358

25 Wang B, Li D, Kovalchuk I, Apel IJ, Chinnaiyan AM, Wóycicki RK, Cantor CR and Kovalchuk O: miR-34a directly targets $tRNA_i^{Met}$ precursors and affects cellular proliferation, cell cycle, and apoptosis. Proc Natl Acad Sci U.S.A. *115(28)*: 7392-7397, 2018. PMID: 29941603. DOI: 10.1073/pnas.1703029115

26 Sherr CJ and DePinho RA: Cellular senescence: mitotic clock or culture shock? Cell *102(4)*: 407-410, 2000. PMID: 10966103. DOI: 10.1016/s0092-8674(00)00046-5

27 Vidale P, Magnani E, Nergadze SG, Santagostino M, Cristofari G, Smirnova A, Mondello C and Giulotto E: The catalytic and the RNA subunits of human telomerase are required to immortalize equid primary fibroblasts. Chromosoma *121(5)*: 475-488, 2012. PMID: 22797876. DOI: 10.1007/s00412-012-0379-4

28 Chen Y, Hu S, Wang M, Zhao B, Yang N, Li J, Chen Q, Liu M, Zhou J, Bao G and Wu X: Characterization and establishment of an immortalized rabbit melanocyte cell line using the SV40 large T antigen. Int J Mol Sci *20(19)*: 4874, 2019. PMID: 31575080. DOI: 10.3390/ijms20194874

29 Ge Y, Smits AM, Liu J, Zhang J, van Brakel TJ, Goumans MJTH, Jongbloed MRM and de Vries AAF: Generation, characterization, and application of inducible proliferative adult human epicardium-derived cells. Cells *10(8)*: 2064, 2021. PMID: 34440833. DOI: 10.3390/cells10082064

30 Kapanadze B, Morris E, Smith E and Trojanowska M: Establishment and characterization of scleroderma fibroblast clonal cell lines by introduction of the hTERT gene. J Cell Mol Med *14(5)*: 1156-1165, 2010. PMID: 19432820. DOI: 10.1111/j.1582-4934.2009.00773.x

31 Nukpook T, Ekalaksananan T, Kiyono T, Kasemsiri P, Teeramatwanich W, Vatanasapt P, Chaiwiriyakul S, Ungarreevittaya P, Kampan J, Muisuk K and Pientong C: Establishment and genetic characterization of cell lines derived from proliferating nasal polyps and sinonasal inverted papillomas. Sci Rep *11(1)*: 17100, 2021. PMID: 34429452. DOI: 10.1038/s41598-021-96444-y

32 Beckenkamp LR, da Fontoura DMS, Korb VG, de Campos RP, Onzi GR, Iser IC, Bertoni APS, Sévigny J, Lenz G and Wink MR: Immortalization of mesenchymal stromal cells by TERT affects adenosine metabolism and impairs their immunosuppressive capacity. Stem Cell Rev Rep *16(4)*: 776-791, 2020. PMID: 32556945. DOI: 10.1007/s12015-020-09986-5

33 Ahuja D, Sáenz-Robles MT and Pipas JM: SV40 large T antigen targets multiple cellular pathways to elicit cellular transformation. Oncogene *24(52)*: 7729-7745, 2005. PMID: 16299533. DOI: 10.1038/sj.onc.1209046

34 Lundberg AS, Randell SH, Stewart SA, Elenbaas B, Hartwell KA, Brooks MW, Fleming MD, Olsen JC, Miller SW, Weinberg RA and Hahn WC: Immortalization and transformation of primary human airway epithelial cells by gene transfer. Oncogene *21(29)*: 4577-4586, 2002. PMID: 12085236. DOI: 10.1038/sj.onc.1205550

35 Gomes RN, Manuel F and Nascimento DS: The bright side of fibroblasts: molecular signature and regenerative cues in major

organs. NPJ Regen Med *6(1)*: 43, 2021. PMID: 34376677. DOI: 10.1038/s41536-021-00153-z

36 Yuan Y, Cruzat VF, Newsholme P, Cheng J, Chen Y and Lu Y: Regulation of SIRT1 in aging: Roles in mitochondrial function and biogenesis. Mech Ageing Dev *155*: 10-21, 2016. PMID: 26923269. DOI: 10.1016/j.mad.2016.02.003

37 Botchkarev VA and Flores ER: p53/p63/p73 in the epidermis in health and disease. Cold Spring Harb Perspect Med *4(8)*: a015248, 2014. PMID: 25085956. DOI: 10.1101/cshperspect.a015248

38 Luo J, Nikolaev AY, Imai S, Chen D, Su F, Shiloh A, Guarente L and Gu W: Negative control of p53 by Sir2alpha promotes cell survival under stress. Cell *107(2)*: 137-148, 2001. PMID: 11672522. DOI: 10.1016/s0092-8674(01)00524-4

39 Langley E, Pearson M, Faretta M, Bauer UM, Frye RA, Minucci S, Pelicci PG and Kouzarides T: Human SIR2 deacetylates p53 and antagonizes PML/p53-induced cellular senescence. EMBO J *21(10)*: 2383-2396, 2002. PMID: 12006491. DOI: 10.1093/emboj/21.10.2383

40 Cullen BR: Transcription and processing of human microRNA precursors. Mol Cell *16(6)*: 861-865, 2004. PMID: 15610730. DOI: 10.1016/j.molcel.2004.12.002

41 Tsai KW, Hu LY, Chen TW, Li SC, Ho MR, Yu SY, Tu YT, Chen WS and Lam HC: Emerging role of microRNAs in modulating endothelin-1 expression in gastric cancer. Oncol Rep *33(1)*: 485-493, 2015. PMID: 25394359. DOI: 10.3892/or.2014.3598

42 Feng S, Gao L, Zhang D, Tian X, Kong L, Shi H, Wu L, Huang Z, Du B, Liang C, Zhang Y and Yao R: MiR-93 regulates vascular smooth muscle cell proliferation, and neointimal formation through targeting Mfn2. Int J Biol Sci *15(12)*: 2615-2626, 2019. PMID: 31754334. DOI: 10.7150/ijbs.36995

43 Zhang C, Zhang Y, Zhu H, Hu J and Xie Z: MiR-34a/miR-93 target c-Ski to modulate the proliferaton of rat cardiac fibroblasts and extracellular matrix deposition *in vivo* and *in vitro*. Cell Signal *46*: 145-153, 2018. PMID: 29551367. DOI: 10.1016/j.cellsig.2018.03.005

44 Chen X, Liu J, Zhang Q, Liu B, Cheng Y, Zhang Y, Sun Y, Ge H and Liu Y: Exosome-mediated transfer of miR-93-5p from cancer-associated fibroblasts confer radioresistance in colorectal cancer cells by downregulating FOXA1 and upregulating TGFB3. J Exp Clin Cancer Res *39(1)*: 65, 2020. PMID: 32293494. DOI: 10.1186/s13046-019-1507-2

45 Li F, Liang X, Chen Y, Li S and Liu J: Role of microRNA-93 in regulation of angiogenesis. Tumour Biol *35(11)*: 10609-10613, 2014. PMID: 25217985. DOI: 10.1007/s13277-014-2605-6

Received August 18, 2021
Revised October 4, 2021
Accepted October 5, 2021